PERSPECTIVE

Quasi-two-dimensional electron gas at the oxide interfaces for topological quantum physics

A Letters Journal Exploring the Frontiers of Physics

January 2021

EPL, **133** (2021) 17001 www.epljournal.org
doi: 10.1209/0295-5075/133/17001

Perspective

Quasi-two-dimensional electron gas at the oxide interfaces for topological quantum physics

A. Barthelemy[1], N. Bergeal[2], M. Bibes[1], A. Caviglia[3], R. Citro[4,5], M. Cuoco[5], A. Kalaboukhov[6], B. Kalisky[7], C. A. Perroni[8], J. Santamaria[9], D. Stornaiuolo[7,10] and M. Salluzzo[10(a)]

[1] *Unité Mixte de Physique, CNRS, Thales, Université Paris-Saclay - F-91767 Palaiseau, France*
[2] *Laboratoire de Physique et d'Etude des Matériaux, ESPCI Paris, PSL Research University, CNRS F-75005 Paris, France*
[3] *Kavli Institute of Nanoscience, Delft University of Technology - P.O. Box 5046, 2600 GA Delft, Netherlands*
[4] *Dipartimento di Fisica "E. R. Caianiello", Università degli Studi di Salerno - I-84084 Fisciano (SA), Italy*
[5] *CNR-SPIN - Via Giovanni Paolo II, 132, I-84084 Fisciano (SA), Italy*
[6] *Department of Microtechnology and Nanoscience-MC2, Chalmers University of Technology SE-41296 Gothenburg, Sweden*
[7] *Department of Physics and Institute of Nanotechnology and Advanced Materials, Bar-Ilan University Ramat-Gan, Israel*
[8] *Dipartimento di Fisica "E. Pancini", Università Federico II di Napoli - Complesso Monte S. Angelo, I-80126 Napoli, Italy*
[9] *GFMC, Departamento de Fisica de Materiales, Universidad Complutense de Madrid - E-28040 Madrid, Spain*
[10] *CNR-SPIN, Complesso Monte S. Angelo - Via Cinthia, I-80126 Napoli, Italy*

received 21 November 2020; accepted in final form 13 January 2021
published online 10 March 2021

PACS 73.20.-r – Electron states at surfaces and interfaces
PACS 74.20.Rp – Superconductivity: Pairing symmetries (other than *s*-wave)
PACS 68.65.-k – Low-dimensional, mesoscopic, nanoscale and other related systems: structure and nonelectronic properties

Abstract – The development of "fault-tolerant" quantum computers, unaffected by noise and decoherence, is one of the fundamental challenges in quantum technology. One of the approaches currently followed is the realization of "topologically protected" qubits which make use of quantum systems characterized by a degenerate ground state of composite particles, known as "non-Abelian anyons", able to encode and manipulate quantum information in a non-local manner. In this paper, we discuss the potential of quasi-two-dimensional electron gas (q2DEG) at the interface between band insulating oxides, like $LaAlO_3$ and $SrTiO_3$, as an innovative technological platform for the realization of topological quantum systems. Being characterized by a unique combination of unconventional spin-orbit coupling, magnetism, and 2D-superconductivity, these systems naturally possess most of the fundamental characteristics needed for the realization of a topological superconductor. These properties can be widely tuned by electric field effect acting on the orbital splitting and occupation of the non-degenerate $3d_{xy}$ and $3d_{xz,yz}$ bands. The topological state in oxide q2DEGs quasi-one-dimensional nanochannels could be therefore suitably controlled, leading to conceptual new methods for the realization of a topological quantum electronics based on the tuning of the orbital degrees of freedom.

Introduction. – The quest for the realization of a universal quantum computer is challenged by the extreme fragility of quantum effects with respect to noise and decoherence. In the last years a growing interest for topological quantum computation emerged, an approach to fault-tolerant qubits based on new states of matter exhibiting topological order and topologically non-trivial electron pairing. In topological qubits the unitary

(a) E-mail: marco.salluzzo@spin.cnr.it

operation results from the braiding of certain quantum objects called "anyons" and satisfying a non-Abelian statistic, like Majorana Zero energy Modes (MZMs) [1]. These new quantum phases are then interesting not only for the fundamental physics, but also for the potential impact on the development of emergent quantum technologies [1–5]. The realization of Majorana states and of non-trivial topological superconductivity (TSC) in condensed matter systems requires the simultaneous presence of three key elements: superconductivity; a breaking of the inversion symmetry, which results in the removal of the spin degeneracy of the electronic bands in momentum space, as it might occur in non-centrosymmetric materials and/or confined systems exhibiting large Rashba spin-orbit coupling (SOC); a source of time-reversal symmetry breaking, like an external magnetic field or a proximity with a ferromagnet, which allows a description of the system by spin-less degrees of freedom.

Research on MZMs-based topological quantum information is currently focused on the superconducting/semiconducting nanowire technology [6–14] however additional materials and platforms have been proposed, as for instance iron-based superconductors, which have shown TSC at their surfaces [15], doped topological insulators [16], two-dimensional (2D) materials and quasi-2D electron gases (q2DEGs) [17].

Several theoretical proposals suggested that the q2DEGs formed at the interface between transition metal oxides (TMO), like $LaAlO_3$ and $SrTiO_3$ (LAO/STO) (fig. 1(a)) [18], are promising candidates for the realization of topological quantum gates based on MZMs in both 2D [19–21] and quasi-one-dimensional (1D) models (fig. 1(b)) [22–26]. These ideas are based on the extraordinary properties of these materials, and in particular the simultaneous presence of strong SOC [27] and 2D-SC [28], both tuneable by electric field effect [27,29]. Moreover, magnetism, coexisting with SC, can be induced by opportune epitaxial engineering [30,31]. All these phenomena are linked to interfacial orbital reconstructions, which dominate the oxide q2DEGs physics [32,33].

The search for TSC in oxide q2DEGs is a new and largely unexplored chapter of condensed matter physics. In this perspective paper, we will describe some recent theoretical studies and experiments aimed at the understanding of the normal and superconducting state of oxide q2DEGs, as fundamental steps for the search of TSC. The second section describes the theoretical TSC phase diagram of nanochannels made of LAO/STO as obtained from self-consistent Hamiltonian calculations based on a realistic band structure of the material. The next section is dedicated to an overview of the common approaches followed to realize LAO/STO nanodevices, of the current challenges and limitations, and we will briefly review experiments on nanobridges, exhibiting Josephson weak coupling, and on quantum dots in the superconducting and in the normal state. In the fourth section, we will give a brief overview of novel oxide q2DEGs of potential interest in the field. Finally, we will conclude this perspective paper by discussing the future steps needed towards the search of TSC in oxide q2DEGs.

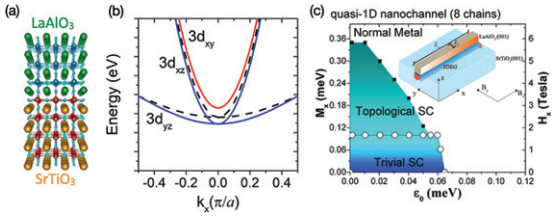

Fig. 1: (a) A sketch of the LAO/STO heterostructure. (b) Electronic band structure near the Fermi level of bulk STO without (black dashed lines) and with SOC included (red line Γ_7^+ doublet and Γ_8^+ quartet). (c) TSC phase diagrams of a LAO/STO nanowire made of 8 chains along the y-direction. The magnetic field is along the wire length (x) (see inset). The magnetic energy (M_x, left) and magnetic field (H_x, right) are plotted as a function of the electron filling, parametrized by ε_0, the energy offset of the Fermi level with respect to the band bottom. In the inset a schematic of a LAO/STO nanowire confined along the y-direction [26].

The topological phase diagram of LAO/STO nanowires. – Despite a simple band structure, the normal and superconducting properties of STO and STO-based heterostructures is very rich. In bulk STO, the $3d$-Ti t_{2g} ($3d_{xy}$, $3d_{xz}$, $3d_{yz}$) manifold (fig. 1(b)) forms the three uppermost bands characterized by heavy and light effective masses along the primitive lattice vectors [34,35]. SOC removes the degeneracy, and the six-fold t_{2g} bands split by about 30 meV in Γ_7^+ doublet and Γ_8^+ quartet [35]. These bands, formed by the mixing of atomic $3d$-Ti t_{2g} states, still retain partially their overall orbital character (fig. 1(b)). In the q2DEG at the (001) LAO/STO interface quantum confinement reverses the bulk orbital hierarchy [32,36], *i.e.*, band with prevalent $3d_{xy}$ character, becomes lower in energy, and it gives rise to several additional subband replicas of $3d_{xy}$ and $3d_{xz,yz}$ orbital characters which mix at various anti-crossing points. At these anti-crossing points several phenomena take place. For example, just below the first anti-crossing, a Lifshitz transition is observed in Hall effect and magnetoresistance measurements, and $3d_{xz,yz}$ carriers start to contribute to the transport properties alongside $3d_{xy}$ carriers [37,38]. Increasing the doping, other anti-crossing points are reached and in some of them evidences for topological band crossing were recently provided in AlO_x/STO heterostructures [39,40]. Among other phenomena, the complex electronic structure and its interplay with the Rashba-like SOC is responsible for an extraordinarily spin-to-charge conversion efficiency in AlO_x/STO and LAO/STO q2DEGs [39,41], larger than the record values of topological insulators like α-Sn [42].

From these general studies, a fundamental role of the multi-orbital nature of the carriers in the electronic properties of the oxide q2DEGs clearly emerges in the 2D limit. It is then expected that SC in quasi-2D and in

particular quasi-1D limits may possess several unconventional properties [22–26].

The TSC phase diagram of LAO/STO q2DEGs nanochannels with lateral sizes from one to 70 chains and length up to 500 atomic sites was recently studied theoretically [26] using a model based on a self-consistent computation of the order parameter as function of the electron filling and of the amplitude of the magnetic field (see ref. [26] for details). The electronic multiband structure of LAO/STO was modelled using a minimal three-bands tight binding model, including the atomic SOC, the inversion (confining) asymmetric potential and the associated orbital Rashba interaction. Confinement gives rise to the formation of several sub-bands which cross at different values of the chemical potential. A magnetic field aligned along the LAO/STO nanowire represents the source of time-reversal symmetry breaking, while SC was modelled assuming conventional intra-orbital spin-singlet s-wave order parameter. Due to the orbital directionality of the t_{2g} states, we find that in the regime of strong confinement the onset of topological phases is pinned close to electron filling where the quasi-flat ($3d_{yz}$) heavy bands start to get populated. It turns out that around these anti-crossing points the density of states has a peak (at the corresponding Van Hove singularities), and both trivial and non-trivial (topological) superconducting regions can be stabilized depending on the external magnetic field (H_x, M_x, along the wire, see inset of fig. 1(c)). This translates in a very intriguing topological phase diagram shown in fig. 1(c) for 8-chains nanowires, with the chemical potential pinned at the first anti-crossing. It emerges that, using realistic parameters, non-trivial topological phase transitions are predicted at magnetic fields of 1.2 (0.5) tesla for 8 (2) chains nanowires, close but still below the parallel critical magnetic field of LAO/STO heterostructures. By increasing the lateral size, up to the superconducting coherence length (70 nm), the TSC phase diagram becomes more complex, with a changeover from a sparse-to-dense distribution of topologically non-trivial domains between trivial superconducting regions, still occurring at the crossovers associated with the orbital population inversion [26].

Thus, these theoretical studies suggest that LAO/STO q2DEGs are promising for the realization of quasi-1D non-trivial topological superconductors. However, some of the intrinsic properties are less favourable. The superconducting T_c is hardly above 250 mK, and it has a gyromagnetic g-factor, ranging from less than 1 to 2.5 [27,43], much smaller than the one of semiconducting nanowires. Furthermore, oxide q2DEGs are subject to some sources of disorder, like oxygen vacancies, which can cause localized magnetic moments and an inhomogeneous landscape of the potential energy, and can heavily influences their properties, including SC and eventual topological excitations.

However, LAO/STO is a 2D superconductor characterized by a large SOC and there is no need to interface the material with other superconductors to get TSC. This is a technological advantage over hybrid superconducting/semiconducting technology, together with the possibility to realize, with a top-down approach, complex device geometries. Additionally, LAO/STO is very sensitive to electrostatic gating and it can be locally tuned from a superconducting to metallic and even insulating states by (side- and top-) gate voltages [43–46].

From a more fundamental perspective, the physics of TMO-based q2DEGs could be the ground for the discovery of new TSC phases with unique characteristics, due to the possible role of electron correlations related to the localized nature of the $3d$-orbital degrees of freedom and their interplay with an unconventional Rashba SOC.

Nanofabrication of LAO/STO q2DEGs quasi-1D channels. – Nanopatterning of oxide q2DEGs needs particular care, and some of the procedures used for the majority of semiconductors, like ion-beam etching, oxygen plasma cleaning and more generally any step involving moderate sample heating, cannot be applied without specific optimization. Here, we briefly review some of the most used methods to realize LAO/STO nanodevices: the atomic force microscopy (AFM) writing of conducting nanochannels; e-beam patterning by amorphous lift-off template, ion-beam irradiation, and local field-effect gating.

The AFM writing technique, developed at the University of Pittsburgh [47,48], is based on the local electric field generated by a conductive AFM tip on samples with a LAO thickness just at the verge of the insulating-to-metal transition (namely 3 unit-cells (uc)), to literally "sketch" non-volatile metallic regions down to few nm widths. However, by their nature these structures do not survive many low-temperature cooling cycles, thus this method is very useful for fundamental physics studies (see for example [49]), but does not allow the realization of nanodevices with long lifetime.

Other approaches are based on e-beam lithography [43–46,50–58], which allows the realization of devices with complex geometries, high yield, and long lifetime. Here we summarize three different approaches for the realization of Josephson Junctions (JJs) [57], SQUID [55] and quantum dots [43,46].

The first method relies on the use of an amorphous template to define the insulating regions on the STO substrate prior to the epitaxial growth of the LAO thin film. Starting from a TiO_2-terminated STO (001) substrate, a resist mask is defined by e-beam lithography. After the development, a thin (10–20 nm) amorphous film (an oxide like LAO, STO or AlO_x) is deposited at room temperature by sputtering or pulsed laser deposition. Using lift-off, the STO areas underneath the resist are cleared out, leaving a "pre-patterned" substrate reproducing the desired shape. On this template, subsequently, epitaxial growth of different complex heterostructures can be carried out, and the device is ready to be tested. This method has the advantage of requiring a single lithographic step and does not

involve manipulation of the q2DEG after its formation. However, even if the STO surface looks well ordered after lift-off, the process can induce subtle changes in the surface termination, which can negatively impact on the properties of the q2DEG nanostructures.

LAO/STO side-gate [44,45] and Dayem bridges behaving as JJs and exhibiting tuneable Josephson effect (fig. 2), have been successfully realized by this method[1] [57]. One of the most intriguing results observed in such Dayem bridges is an anomaly of the Josephson critical current *vs.* magnetic field pattern, $I_c(H)$, shown in fig. 2(b), which exhibits a dip at zero magnetic field. This anomaly was observed for various gate voltages, *i.e.*, carrier densities, from the underdoped to the slightly overdoped regime tuned by back-gate voltages. The anomalous pattern was interpreted as a possible signature of an unconventional component of the order parameter giving rise to a π-channel (π being the phase difference across the junction) in parallel to a standard 0-channel. Possible scenarios which can explain these results include a mixed s-wave and triplet order parameter, which would be present due to the strong Rashba-like SOC, or other unconventional order parameters, like the recently proposed $s\pm$ pairing [59].

An alternative route to pattern LAO/STO q2DEGs was proposed by the Chalmers group [52,53,56,58]. The method is based on Ar-ion beam irradiation that induces an insulating state due to Ar-implantation in the LAO film [52,53]. The use of low energy and short irradiation times is crucial to avoid formation of oxygen vacancies in the STO substrate.

This method does not require hard masks or aggressive chemicals, and the dimensions of fabricated structures are limited only by the e-beam lithography-defined mask used to protect the areas which will form the conductive part of the devices. Figures 2(c)–(d) show examples of nanostructures with dimensions below 100 nm fabricated using this method, while in fig. 2(e) I *vs.* V data demonstrate homogeneous superconductivity in nanostructures with linewidths down to 70 nm [58].

A third approach is based on the large sensitivity of oxide q2DEGs to electric field effect. As mentioned above, a superconducting-to-insulating transition can be achieved with moderate gate voltages. Thus, superconducting nanodevices can be realized using, locally, either top-gates (to deplete the region underneath) or split-gates (to deplete the oxide q2DEGs everywhere outside the region of interest). The realization of LAO/STO nanostructures using top- and split-gates methods was developed at TU-Delft [54,55]. First, a LAO/STO microbridge is realized by the amorphous template method to define the general layout. Then, high-resolution e-beam lithography is used to realize metallic gate electrodes on top of the LAO film in the position defined by tungsten markers previously created on the substrate. Finally, a metallic back-gate is deposited

[1]In a Dayem bridges, a weak Josepshon coupling between two superconducting banks is achieved through a constriction with size comparable to the coherence length ξ (for LAO/STO $\xi \approx 50$–70 nm).

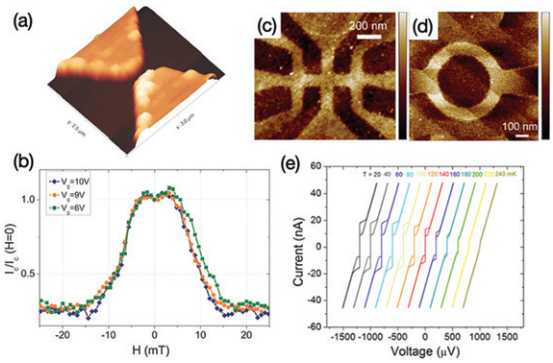

Fig. 2: (a) AFM image of a 200 nm (width and length) LAO/STO Dayem bridge. Darker areas are the regions where the q2DEG is formed. (b) Anomalous $I_c(H)$ pattern. (c), (d): AFM images of LAO/STO nanostructures patterned using low-energy Ar+ ion-beam irradiation: (c) Hall bar with a linewidth of 100 nm; (d) ring with a linewidth of 100 nm and inner diameter of 400 nm. (e) Current-voltage characteristics of the nanoring in the 20–240 mK range.

on the back side of STO, enabling a global control of the electron density, as in the devices shown in fig. 3 and fig. 4. Split-gate structures were used to realize Superconducting Quantum Point Contacts (SQPC) [46]. With a separation between gates of $\sim$150 nm, *i.e.*, of the order of the in-plane superconducting coherence length and of the normal state phase correlation length, the device enters at low temperature a quantum transport regime. As a function of the electrostatic gating three distinct regimes can be accessed (fig. 3(c)): i) a weak link regime with a supercurrent carried by quantized modes (SQPC) with a large (60%) transmittivity, consistent with the pure electrostatic nature of the NS interfaces. ii) a superconducting quantum dot regime with even-parity transport (Cooper pair) below the superconducting gap and odd-parity transport (quasiparticle) above, iii) a normal state island coupled to superconducting reservoirs, with a quantum level spacing of the order of the superconducting gap. This device design is a tuneable platform for bound states spectroscopy at the edge of 1D channels.

Using a similar approach, LAO/STO Quantum Point Contact (QPC) devices, with separation between the two fingers at the center of a split-gate of $w = 25$ nm (comparable to the Fermi wavelength, λ_F, of the q2DEG) (fig. 4), were fabricated by the ESCPI group [43]. Near the bottleneck of the constriction, the split-gate imposes a smoothly varying confining potential in the transverse direction. Figure 4(c) shows the evolution of the conductance at zero source-drain voltage as a function of the split-gate voltage V_{SG}. At $V_{SG} = -0.2$ V the QPC is pinched off. Plateaus, corresponding to integer values of the $G_0 = 2e^2/h$ conductance, appear when V_{SG} is increased, which indicates ballistic transport involving spin-degenerated bands in the QPC. Three plateaus can be identified in this gate range, corresponding to $\lambda_F \approx 15$ nm. Under a magnetic field

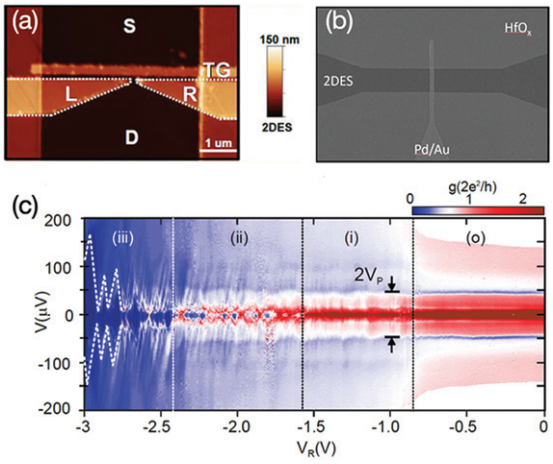

Fig. 3: (a) AFM of a split- and top-gate device realized with a combination of hard mask and electron beam lithography. (b) SEM imaging of a structure with top-gate lateral size of ∼150 nm. (c) Various transport regimes of a split gated structure measured at $T = 40$ mK and spatial confinement of the order of 150 nm.

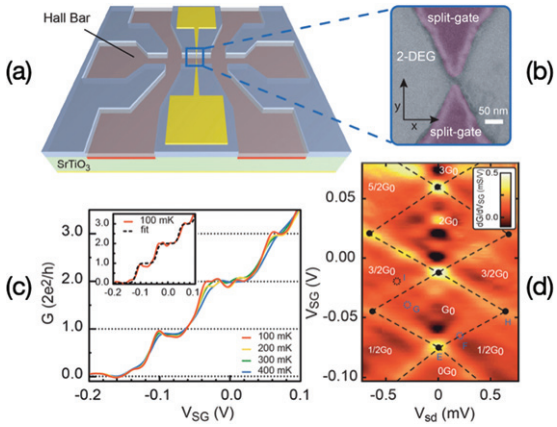

Fig. 4: (a) Scheme of the QPC device in a $LaAlO_3/SrTiO_3$ interface. (b) SEM image of the QPC. (c) Quantization of conductance in integer values of $2e^2/h$. (d) Spectroscopy of the energy levels obtained by measuring the transconductance of the device (colour code) as a function of source-drain voltage and split-gate voltage. Each diamond represents a well-defined quantized conductance.

spin-polarized sub-bands are formed, corresponding to a g-factor, estimated from the conductance spectroscopy of the $3d$-levels (fig. 4(d)), of $g \approx 0.9$ [43], in agreement with previous estimates for LAO/STO q2DEGs at low doping [27].

Recently, QPC superconducting devices were realized also on the STO surface doped by ionic liquid gating. These devices show a quantization of the superconducting critical current as a function of the split-gate voltage, which is interesting for the investigation of MZMs modes [60].

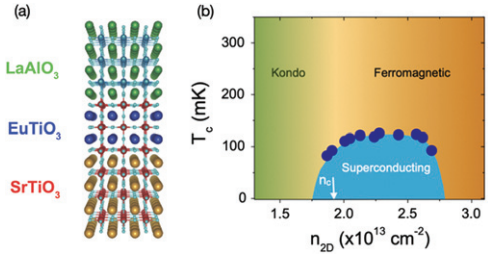

Fig. 5: (a) Sketch of a LAO/ETO/STO heterostructure. (b) Phase diagram of the LAO/ETO/STO heterostructure, showing Kondo and ferromagnetic regions in the normal state, and a low-temperature superconducting state in a large range of doping.

Novel engineered heteostructures. – The intense research activity on LAO/STO heterostructures has, in the course of time, brought to several fascinating and unexpected results, which enlarged the interest in oxide q2DEGs and boosted the research towards possible applications. One of the most unexpected properties, reported few years after its discovery, was the observation of magnetic effects at this interface. Being both LAO and STO non-magnetic, this result came as a surprise and several groups tried to clarify the nature of the magnetism and its origin [33,61,62]. Now it is well established that the LAO/STO q2DEG is not intrinsically spin-polarized, and signatures of magnetism (if any) are weak and generally related to oxygen vacancies which induce localized Ti^{3+} magnetic moments. For this reason, other oxide interfaces which could host q2DEGs showing a robust spin-polarization were investigated. A viable route in these directions is the introduction of a very thin layer of a magnetic oxide between LAO and STO or the replacement of LAO with a ferromagnetic insulator [30,31,63].

Among these heterostructures, one of the most intriguing is the $LaAlO_3/EuTiO_3/SrTiO_3$ (LAO/ETO/STO) trilayer, where a thin (2 uc) epitaxial film of $EuTiO_3$ (ETO) is inserted between LAO and STO (fig. 5(a)). The q2DEG formed thereby shows an electric field tuneable ferromagnetism and spin-polarization below 6–8 K, coexisting with Rashba-like SOC [64] and with SC below 150 mK [31]. The ferromagnetism and the SC are tuneable by gate voltages, which result in an intriguing phase diagram (fig. 5(b)), where a transition from a ferromagnetic to a superconducting state is observed. The three ingredients together, *i.e.*, magnetism, superconductivity and spin-orbit coupling, fully tuneable by electric field effect, make the LAO/ETO/STO system an exceptional platform for the investigation of novel quantum states of matter and of topological superconductivity [5,31].

Another method to induce or enhance topological effects is by replacing STO with oxides characterized by larger atomic spin-orbit coupling. Following these directions, iridates heterostructures characterized by a very large SOC, owing to the Ir-5d carriers [65], have been

realized. Unfortunately, these heterostructures do not show evidences of superconductivity, however they can be considered as the oxide analogous of semiconducting nanowires. Thus, proximitized by another superconductor, they could exhibit TSC.

Along the same directions, researchers are studying q2DEGs in $KTaO_3$ heterostructures. (001) $KTaO_3$ shows a maximum T_c of 60 mK at large doping induced by ionic liquid gating. However, recently T_c up to 2 K were reported in (111) $KTaO_3$ at the interface with polycrystalline EuO or amorphous $LaAlO_3$ [66]. As the atomic spin-orbital splitting of this heterostructures is up to 0.5 eV, this system is very promising for the search of TSC phases. The fact that T_c increases so much only by changing the crystallographic direction of the interface is very intriguing, and it is just one of the latest surprises that oxide interface physics gave in the last few years.

Final remarks and perspectives. – The search for TSC in oxide q2DEGs is only at the beginning, and several crucial steps have to be taken in the next future. First of all, a complete comprehension of the electronic properties of these materials is needed, in particular for what concerns the interplay between SC, SOC and the multiband-orbital physics. In the last few years, many efforts were devoted to the understanding of the mechanism leading to the formation of a q2DEG at the interface of oxide band insulator. The frontier of the research in the field is now mastering the properties of these oxide q2DEGs, in both 2D and quasi-1D nanodevices, performing the right experiments addressing their fundamental properties, and finally achieving a control of these properties by external stimuli, like electric field effect, magnetic field and heterostructure engineering. There are important fundamental issues that need to be addressed and properties to be controlled. For example, the domain structure of STO at low temperature, induced by the cubic-to-tetragonal transition of the crystal structure, has an impact in the microscopic transport properties of the q2DEG, as shown by Scanning Squid Microscopy studies which detected enhanced current at the domain walls (fig. 6(a) and ref. [67]). These conduction paths, while representing interesting intrinsic few nm nanochannels for the transport, also provide a challenge for the realization of nanodevices with homogeneous properties.

A better understanding of the complex physics underlying the properties of oxide q2DEGs, including the effect of electron correlations, should now be coupled to the design of devices and experiments targeted at addressing TSC and proving the existence of MZMs modes, which is challenging. Tunnelling experiments, in normal/superconducting oxide q2DEGs junctions, are possible with a metallic electrode placed on top of the insulating LAO layer which acts as tunnelling barrier [68,69]. However, due to the strong confinement of the q2DEG and to the large minimum barrier thickness, in-plane

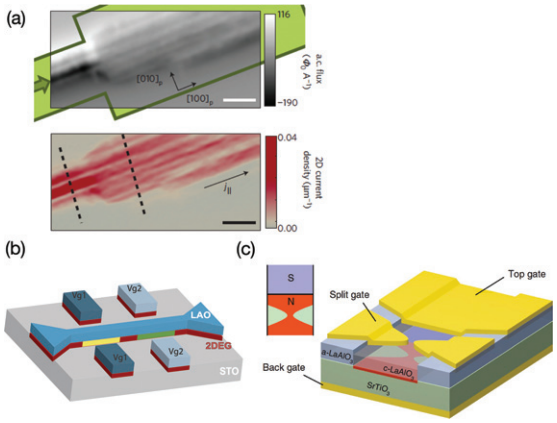

Fig. 6: (a) (Top) Magnetic flux image in patterned LAO/STO sample (green outline), and (bottom) reconstructed current densities along the device, showing the presence of high current density paths (from ref. [67]). (b) Layout of a side-gates device allowing the individual control of two sections of a LAO/STO nanochannel for in-plane tunnelling experiments. (c) Prototype device for the detection of Majorana states in LAO/STO interfaces with a QPC (from ref. [43]). An additional top-gate is used to create, close to the QPC, a superconducting region (S) and a normal one (N).

tunnel junctions are needed at the nanoscale to probe the full density of states with sufficient sensitivity. One approach to perform such experiments is to create a non-superconducting region in a part of a channel and control the superconducting properties of the other by local gates, as shown in fig. 6(b). Besides tunnelling experiments, in order to prove TSC, there is a need to combine several experiments, like the study of the order parameter symmetry using phase sensitive experiments employing JJs with different geometrical configurations. For example, information about the possible presence of MZMs in nanodevices can be obtained by looking at the Shapiro steps periodicity in oxide q2DEGs JJs.

Probably, the most interesting proposal in these directions is the Wimmer *et al.* and Bennaker idea [70,71]. When a QPC is placed nearby a non-trivial topological superconducting region, (fig. 6(c), inset), the conductance plateaus should appear at $(2n+1)\ 2e^2/h$ values. In this case, the current flows through a Majorana state localized in the vicinity of the QPC. The $n = 0$ half-integer plateau at a conductance of $2e^2/h$ is topologically protected against disorder and is expected to provide a robust distinctive signature of the topological phase. Following this idea, a prototype device for the detection of Majorana states in LAO/STO interfaces with a QPC (fig. 6(c)) was proposed in ref. [43]. Here, the split-gate controls the QPC conductance in the quantized regime, which is reached by depletion of the q2DEG with the back-gate. An additional top-gate would then be used to induce superconductivity in the oxide q2DEG by doping, and hence create a non-trivial topological superconducting region in the vicinity of the QPC.

In conclusion, in this perspective paper we have described some of the recent theoretical and experimental developments towards the understanding of the normal and superconducting state of oxide q2DEGs, as fundamental steps for the search of topological states. In oxide q2DEGs, with their unique combination of tuneable SOC, superconductivity and magnetism, the physics of a confined electron systems meets the fascinating world of transition metal oxides and of electron correlated materials. Even if the road towards possible quantum applications is very long, both theoretical and experimental developments in the field provide promises in the right directions.

* * *

This project received funding from the ERA-NET QUANTERA European Union's Horizon H2020 project QUANTOX under Grant Agreement No. 731473, from the Ministero dell'Istruzione, dell'Università e della Ricerca for the PRIN project TOP-SPIN (Grant No. PRIN 20177SL7HC), the ERC Advanced grant No. 833973 "FRESCO".

REFERENCES

[1] Das Sarma S., Freedman M. and Nayak C., *npj Quantum Inf.*, **1** (2015) 1.
[2] Shen S.-Q., *Topological Insulators - Dirac Equation in Condensed Matters* (Springer, Berlin) 2012.
[3] Bernevig B. A., *Topological Insulators and Topological Superconductors* (Princeton University Press, Princeton, NJ) 2013.
[4] Qi X.-L. and Zhang S.-C., *Rev. Mod. Phys.*, **83** (2011) 1057.
[5] Sato M. and Ando Y., *Rep. Prog. Phys.*, **80** (2017) 076501.
[6] Kitaev A. Y., *Phys. Usp.*, **44** (2001) 131.
[7] Lutchyn R. M., Sau J. D. and Das Sarma S., *Phys. Rev. Lett.*, **105** (2010) 077001.
[8] Oreg Y., Refael G. and von Oppen F., *Phys. Rev. Lett.*, **10** (2010) 177002.
[9] Aguado R., *Riv. Nuovo Cimento*, **40** (2017) 523.
[10] Mourik V. *et al.*, *Science*, **336** (2012) 1003.
[11] Albrecht S. M. *et al.*, *Nature*, **531** (2016) 206.
[12] Deng M. T. *et al.*, *Science*, **354** (2016) 1557.
[13] Zhang H. *et al.*, *Nature*, **556** (2018) 74.
[14] Lutchyn R. M. *et al.*, *Nat. Rev. Mater.*, **3** (2018) 52.
[15] Zhang P. *et al.*, *Science*, **360** (2018) 182.
[16] Wray L. A. *et al.*, *Nat. Phys.*, **6** (2010) 855.
[17] Fornieri A. *et al.*, *Nature*, **569** (2019) 855.
[18] Ohtomo A. and Hwang H. Y., *Nature*, **427** (2004) 423.
[19] Mohanta N. and Taraphder A., *EPL*, **108** (2014) 60001.
[20] Scheurer M. S. and Schmalian J., *Nat. Commun.*, **6** (2015) 6005.
[21] Fukaya Y. *et al.*, *Phys. Rev. B*, **97** (2018) 174522.
[22] Sau J. D. *et al.*, *Phys. Rev. Lett.*, **104** (2010) 040502.
[23] Fidkowski L. *et al.*, *Phys. Rev. B*, **84** (2011) 195436.
[24] Fidkowski L., Jiang H.-C., Lutchyn R. M. and Nayak C., *Phys. Rev. B*, **87** (2013) 014436.
[25] Mazziotti M. V., Scopigno N., Grilli M. and Caprara S., *Condens. Matter*, **3** (2018) 37.
[26] Perroni C. A. *et al.*, *Phys. Rev. B*, **100** (2019) 094526.
[27] Caviglia A. D. *et al.*, *Phys. Rev. Lett.*, **104** (2010) 126803.
[28] Reyren N. *et al.*, *Science*, **317** (2007) 1196.
[29] Caviglia A. D. *et al.*, *Nature*, **456** (2008) 624.
[30] De Luca G. M. *et al.*, *Phys. Rev. B*, **89** (2014) 224413.
[31] Stornaiuolo D. *et al.*, *Nat. Mater.*, **15** (2016) 278.
[32] Salluzzo M. *et al.*, *Phys. Rev. Lett.*, **102** (2009) 166804.
[33] Salluzzo M. *et al.*, *Phys. Rev. Lett.*, **111** (2013) 087204.
[34] Mattheiss L. F., *Phys. Rev. B*, **6** (1972) 4740.
[35] Zhong Z., Toth A. and Held K., *Phys. Rev. B*, **87** (2013) 161102.
[36] Cancellieri C. *et al.*, *Phys. Rev. B*, **89** (2014) 121412.
[37] Joshua A. *et al.*, *Nat. Commun.*, **3** (2012) 1129.
[38] Diez M. *et al.*, *Phys. Rev. Lett.*, **115** (2015) 016803.
[39] Vaz D. C. *et al.*, *Nat. Mater.*, **39** (2019) 78.
[40] Vivek M., Goerbig M. O. and Gabay M., *Phys. Rev. B*, **95** (2017) 165117.
[41] Lesne E. *et al.*, *Nat. Mater.*, **15** (2016) 1261.
[42] Rojas-Sánchez J. C. *et al.*, *Phys. Rev. Lett.*, **116** (2016) 096602.
[43] Jouan A. *et al.*, *Nat. Electron.*, **3** (2020) 201.
[44] Stornaiuolo D. *et al.*, *Phys. Rev. B*, **90** (2014) 235426.
[45] Monteiro A. M. R. V. L. *et al.*, *Nano Lett.*, **17** (2017) 715.
[46] Thierschmann H. *et al.*, *Nat. Commun.*, **9** (2018) 2276.
[47] Cen C. *et al.*, *Science*, **323** (2009) 1026.
[48] Pai Y.-Y., Tylan-Tyler A., Irvin P. and Levy J., *Rep. Prog. Phys.*, **81** (2018) 036503.
[49] Cheng G. *et al.*, *Nature*, **521** (2015) 196.
[50] Schneider C. W. *et al.*, *Appl. Phys. Lett.*, **89** (2006) 12210.
[51] Stornaiuolo D. *et al.*, *Appl. Phys. Lett.*, **101** (2012) 222601.
[52] Aurino P. P. *et al.*, *Appl. Phys. Lett.*, **102** (2013) 201610.
[53] Aurino P. P. *et al.*, *Phys. Rev. B*, **92** (2015) 155130.
[54] Goswami S. *et al.*, *Nano Lett.*, **15** (2015) 2627.
[55] Goswami S. *et al.*, *Nat. Nanotechnol.*, **11** (2016) 861.
[56] Aurino P. P. *et al.*, *Phys. Rev. Appl.*, **6** (2016) 024011.
[57] Stornaiuolo D. *et al.*, *Phys. Rev. B*, **95** (2017) 140502.
[58] Kalaboukhov A. *et al.*, *Phys. Rev. B*, **96** (2017) 184525.
[59] Singh G. *et al.*, *Nat. Mater.*, **18** (2019) 948.
[60] Mikheev E., Rosen I. T. and Goldhaber-Gordon D., arXiv:2010.00183 (2020).
[61] Bert J. A. *et al.*, *Nat. Phys.*, **7** (2011) 767.
[62] Lee J. S. *et al.*, *Nat. Mater.*, **12** (2013) 703.
[63] Zhang H. R. *et al.*, *Phys. Rev. B*, **96** (2017) 195167.
[64] Stornaiuolo D. *et al.*, *Phys. Rev. B*, **98** (2018) 075409.
[65] Groenendijk D. J. *et al.*, *Phys. Rev. Lett.*, **119** (2017) 256403.
[66] Liu C. *et al.*, *Science*, **371** (2021) 716.
[67] Kalisky B. *et al.*, *Nature*, **12** (2013) 1091.
[68] Richter C. *et al.*, *Nature*, **502** (2013) 528.
[69] Kuerten L. *et al.*, *Phys. Rev. B*, **96** (2017) 75.
[70] Wimmer M. *et al.*, *New J. Phys.*, **13** (2011) 053016.
[71] Beenakker C. W. J., *Annu. Rev. Condens. Matter Phys.*, **4** (2013) 113.